# Supporting Information

## Salio et al. 10.1073/pnas.1413935112

### SI Materials and Methods

**Medium and Reagents.** The complete medium (CM) used throughout was RPMI 1640 (Gibco) for dendritic cells and Iscove's modified Dulbecco's medium (Gibco) for human iNKT cells. CM was supplemented with 2 mM L-glutamine, 1% nonessential amino acids, 1% sodium pyruvate, 1% penicillin/streptomycin, $5 \times 10^{-5}$ M2ME (beta mercaptoethanol) (all from Gibco) and serum: 10% (vol/vol) FCS (Sigma) or 5% (vol/vol) human AB serum (Sigma) for iNKT cells. Recombinant human IL-2 was produced in our laboratory as described (1).

**Lipids.** α-GalCer and Gal(α1→2)GalCer were synthesized by a strategy described previously (2–4), and their structures were confirmed by mass spectrometry. The dried lipids were dissolved at 10 mg/mL in a solution of chloroform:methanol:water (10:10:3; vol/vol/vol), followed by dilution in 150 mM NaCl, 0.5% Tween 20 (vehicle solution) at 100–200 μg/mL stock solution (depending on solubility). The solution was heated at 80 °C for 5 min followed by sonication for 5 min in an ultrasonic water bath.

**Tetramers.** Human CD1d and β2M proteins were expressed in *Escherichia coli* as inclusion bodies and refolded around α-GalCer using in vitro oxidative chromatography as described (5). For the experiments shown in Fig. S2, recombinant mouse CD1d negative control tetramers (E002-2A-G) and α-GalCer–loaded recombinant murine CD1d tetramers (E001-2A-G) were purchased from Proimmune.

**Probes.** A Cyto ID Autophagy Detection kit (Enzo Life Sciences) was used at 5 μM final concentration, according to the manufacturer's instructions. MitoTracker and MitoSox (both from Molecular Probes) were used at 150 nM and 5 μM, respectively, in complete serum-free medium for 30 min in a 37° incubator with 5% $CO_2$. Apoptosis was measured with antibodies to Annexin V in Annexin-binding buffer (BD Pharmingen) after culturing the cells in complete medium for 4 h in a 37° incubator with 5% $CO_2$. 6-NBDG (Molecular Probes) was resuspended in DMSO at 10 mM and used at a final concentration of 100 μM in complete serum-free medium for 30 min in a 37° incubator with 5% $CO_2$.

**Antibodies for Flow Cytometry.** Antibodies were purchased from eBiosciences (CD4, clone GK1.5; γδ TCR, clone GL3; Ki67, clone SolA15; CD44, clone IM7; CD3, clone 2C11; TCRβ, clone H57-597; Bcl2, clone 10C4; CD24, clone M1/69; CD45.1, clone A20; CD45.2, clone 104; IFNγ, clone XMG1.2; IL-4, clone 11B11; Vβ8.1/b.2, clone KJ16-133; CD11c, clone N418; CD11b, clone M1/70; CD1d, clone 1B1; ICOS, clone 7E.17G9; RORγt, clone B2D; T-bet, clone 4B10; Egr-2, clone erongr2) or from Biolegend (CD69, clone H1.2F3; CD8a, clone 53–6.7; PLZF, clone 9E12; CD62L, clone MEL-14; NK1.1, clone PK136; B220, clone RA3-6B2). Anti–Glut-1 antibody, clone 202915, was from R&D Systems. Samples were acquired on an LSRII analyzer, and data were processed with Flowjo 9. For analysis, all samples were sequentially gated on small lymphocytes, singlets, and live cells, after which B cells were excluded to reduce nonspecific α-GalCer CD1d tetramer binding.

**RNA Extraction and qPCR.** RNA was extracted from sorted cells with RNAeasy columns (Qiagen) and quantified with a Nanodrop Spectrophotometer. cDNA was synthesized from 200 ng of RNA using the High-Capacity cDNA Archive kit (Applied Biosystems). Real-time quantitative PCR was performed in duplicate on the Applied Biosystems 7500 Fast Real-Time PCR system, according to the manufacturer's instructions, and using Applied Biosystems Taqman Universal PCR Master mix and Taqman probes. Analysis of gene expression was calculated according to the $2^{-\Delta Ct}$ method using HPRT as the housekeeping gene. HPRT and Atg7 Taqman probes were from Applied Biosystems.

To detect Vα14–Jα18 rearrangements, RNA was extracted from $8 \times 10^6$ sorted DP thymocytes depleted of α-GalCer-CD1d tetramer$^+$ cells. The sequences of the primers and Taqman probes used in this analysis have been previously published by Gapin et al. (6) and are as follows: Vα14—5′-TGGGAGATACTCAGCAACTCTGG-3′; Jα18—5′-CAGGTATGACAATCAGCTGAGTCC-3′; Cα forward—5′-CCTCTGCCTGTTCACCGACTT-3′; Cα reverse—5′-TGGCGTTGGTCTCTTTGAAG-3′; Vα-14 PROBE FAM—5′-FAM-CACCCTGCTGGATGACACTGCCAC-TAMRA-3′; and Cα-PROBE FAM—5′-FAM-CTCCCAAATCAATGTGCCGAAAACCA-TAMRA-3′.

Analysis of gene expression was calculated according to the $2^{-\Delta Ct}$ method using Cα amplicons as a reference.


1. Traunecker A, Oliveri F, Karjalainen K (1991) Myeloma based expression system for production of large mammalian proteins. *Trends Biotechnol* 9(4):109–113.
2. Jervis PJ, et al. (2010) Synthesis and biological activity of alpha-glucosyl C24:0 and C20:2 ceramides. *Bioorg Med Chem Lett* 20(12):3475–3478.
3. Veerapen N, et al. (2009) Synthesis and biological activity of alpha-galactosyl ceramide KRN7000 and galactosyl (alpha1→2) galactosyl ceramide. *Bioorg Med Chem Lett* 19(15):4288–4291.
4. Wojno J, et al. (2012) Amide analogues of CD1d agonists modulate iNKT-cell-mediated cytokine production. *ACS Chem Biol* 7(5):847–855.
5. Karadimitris A, et al. (2001) Human CD1d-glycolipid tetramers generated by in vitro oxidative refolding chromatography. *Proc Natl Acad Sci USA* 98(6):3294–3298.
6. Hager E, Hawwari A, Matsuda JL, Krangel MS, Gapin L (2007) Multiple constraints at the level of TCRalpha rearrangement impact Valpha14i NKT cell development. *J Immunol* 179:2228–2234.

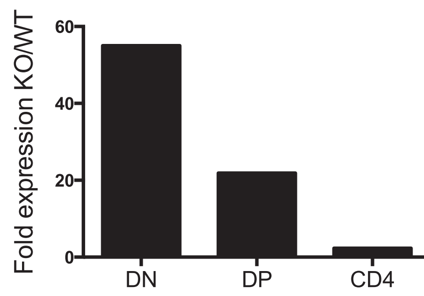


**Fig. S1.** Deletion of *Atg7* in CD4 Cre-Atg7$^{-/-}$ mice. *Atg7* expression levels as determined by qPCR in knockout mice relative to a WT counterpart for each sorted thymic population.

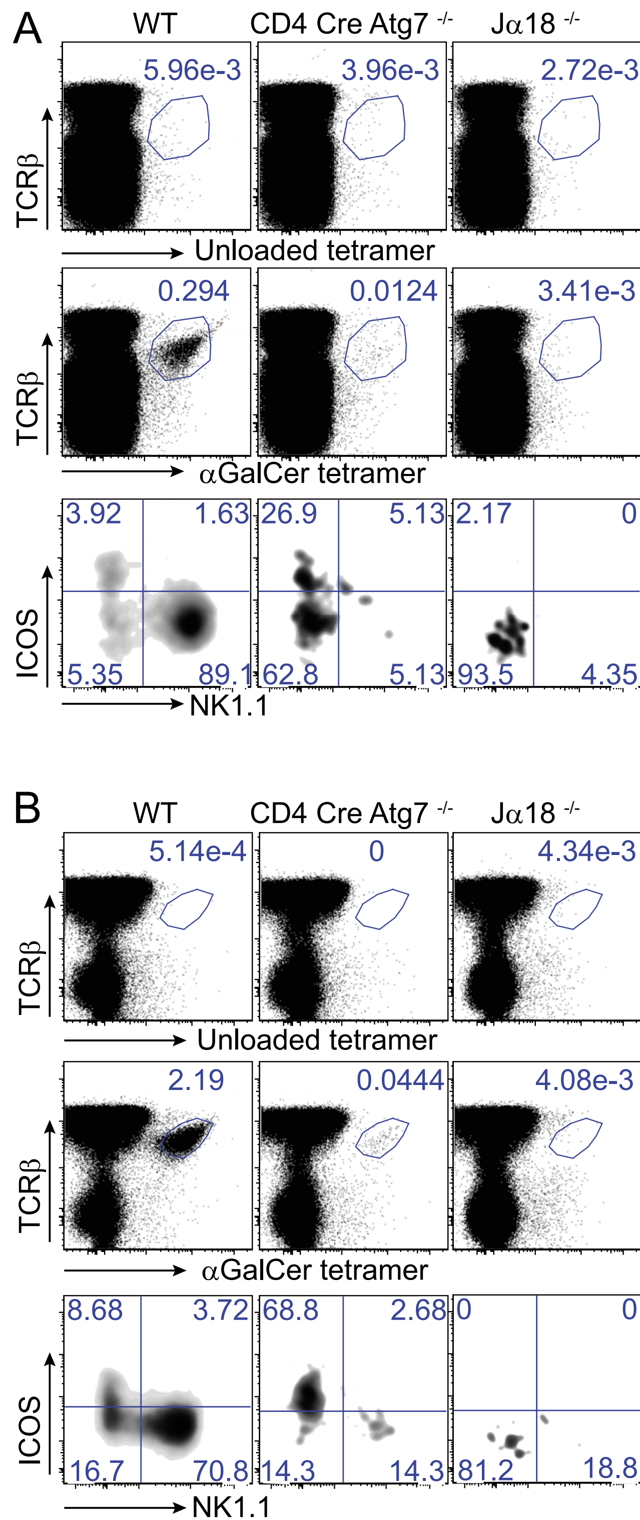


**Fig. S2.** Representative FACS dot plots depicting thymic (*A*) and splenic (*B*) iNKT cell frequencies and phenotype. For each panel, the top row represents staining with unloaded CD1d tetramers and the middle row staining with α-GalCer–loaded CD1d tetramers. (*Bottom*) The expression of ICOS and NK1.1 on the gated iNKT cells (TCRβ$^+$ αGalCer-CD1d$^+$ cells). One representative mouse per group (one experiment representative of three with two to three mice per group).

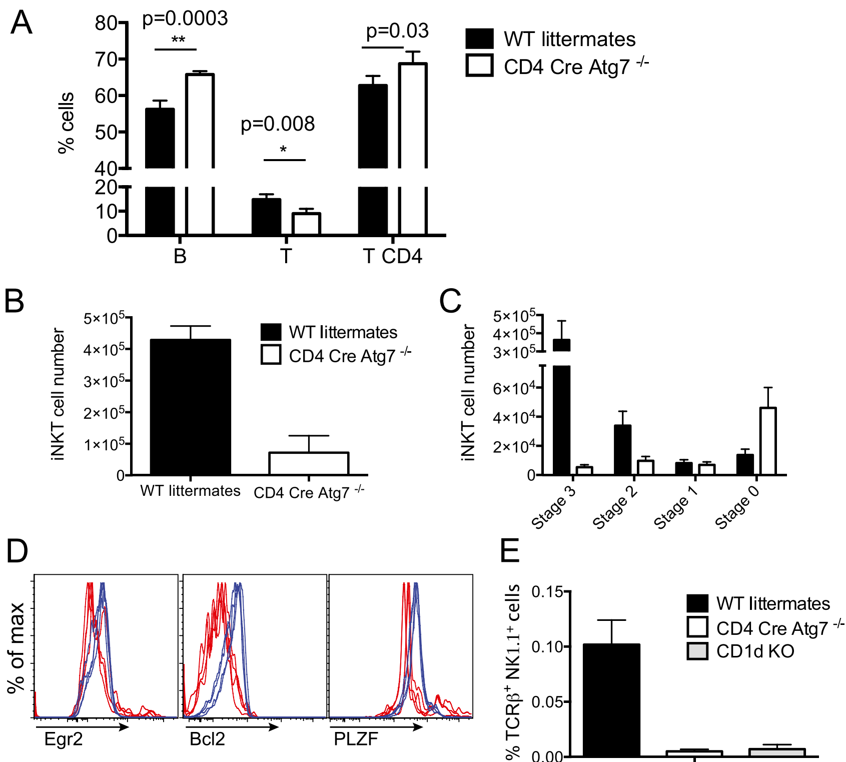


**Fig. S3.** (*A*) Percentages of B, T, and CD4 T cells (mean ± SD) in the spleen of WT or Cre-Atg7$^{-/-}$ mice. As CD4 T-cell percentages are increased, there is a mirror reduction in the percentage of CD8 T cells. $n = 4$ mice/group. (*B* and *C*) Absolute quantification of (*B*) total thymic iNKT cell numbers and (*C*) numbers at each of the maturation stages defined in Fig. 2*D*. Mean ± SEM; $n = 8$ WT and 6 CD4 Cre-Atg7$^{-/-}$ mice. (*D*) Intracellular expression of Egr2, Bcl2, and PLZF in gated thymic iNKT cells in WT and CD4 Cre-Atg7$^{-/-}$ mice. Overlays of four WT (blue) and four CD4 Cre-Atg7$^{-/-}$ mice (red). In CD4 Cre-Atg7$^{-/-}$ mice, a small population is present expressing higher PLZF, and these cells are stage 1 iNKT cells. (*E*) Frequencies of thymic type II iNKT cells defined as CD1d-αGalCer tetramer$^{-}$ TCRβ$^{+}$ NK1.1$^{+}$ cells. $n = 8$ mice/group from two independent experiments.

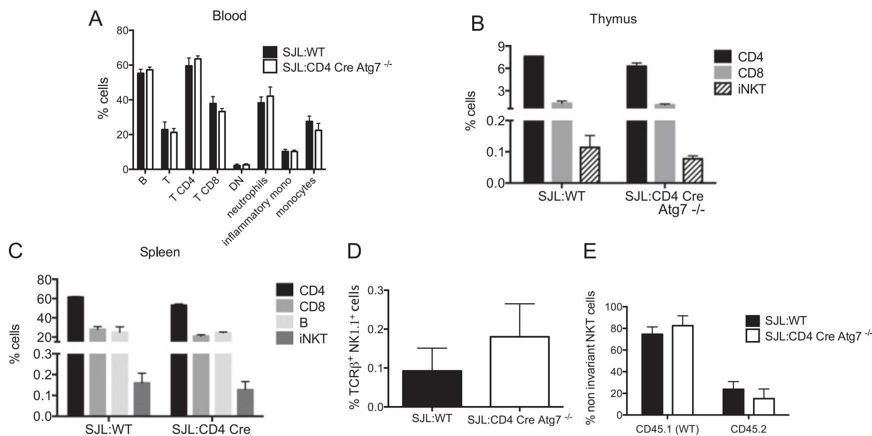


**Fig. S4.** Analysis of the reconstitution of bone marrow chimeric mice. CD45.2 BM cells from WT or CD4 Cre-Atg7$^{-/-}$ were mixed 1:1 with CD45.1 SJL (WT) BM cells and transplanted into lethally irradiated CD45.1 SJL WT recipients ($n = 4$/group). Nine weeks after the percentages of cells (mean ± SD) were determined in peripheral blood (*A*), thymus (*B*), and spleen (*C*) for control (SJL:WT) and SJL:CD4 Cre-Atg7$^{-/-}$ chimeras. Also shown are the percentages of noninvariant NKT cells in the two chimeras (*D*) and the contribution of each donor population toward their reconstitution (*E*).

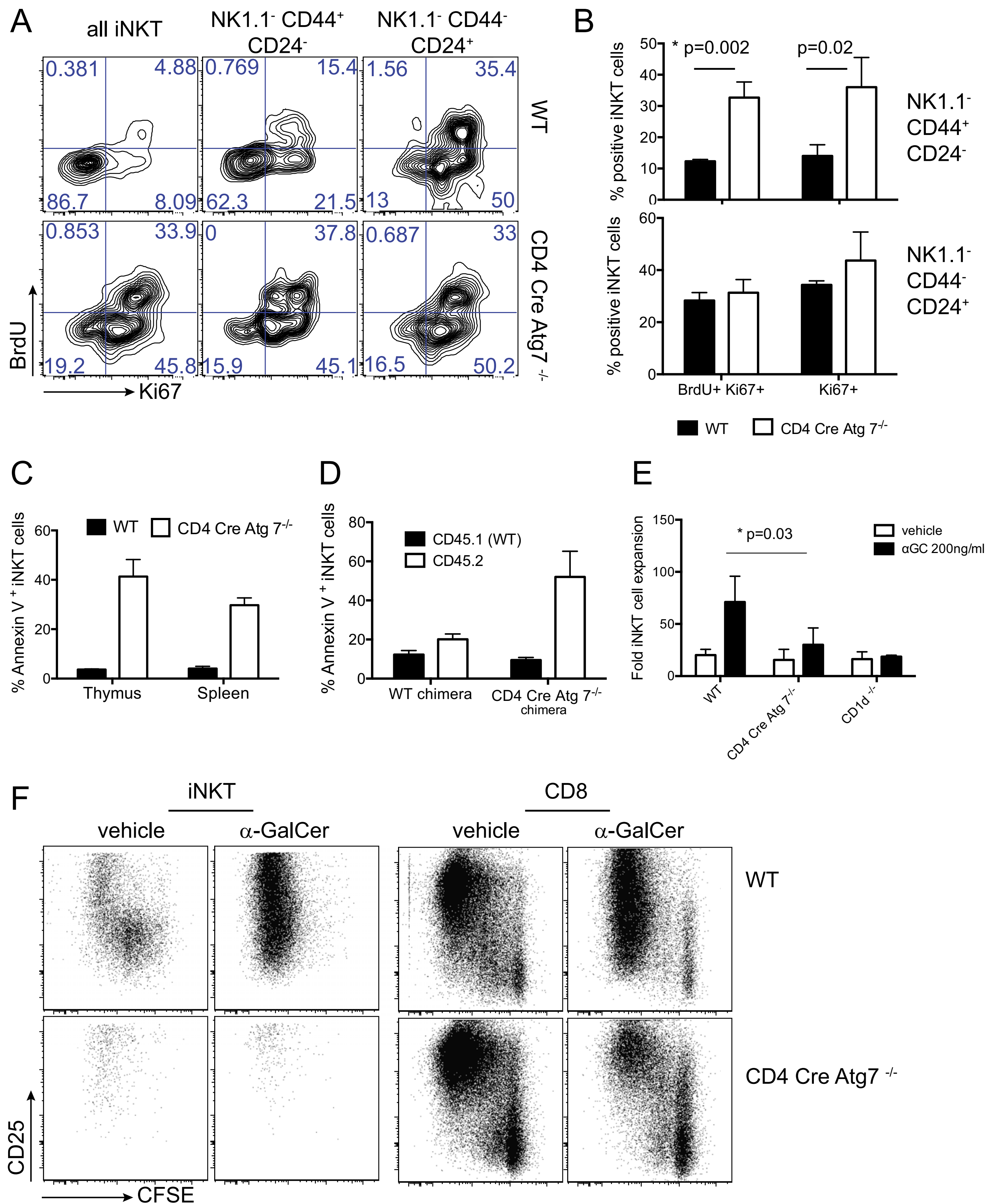


**Fig. S5.** (*A* and *B*) Enhanced BrdU incorporation in CD4 Cre-Atg7$^{-/-}$ iNKT cells. Thymic total iNKT cells and the NK1.1$^{-}$ CD44$^{+}$ CD24$^{-}$ and the NK1.1$^{-}$ CD44$^{-}$ CD24$^{+}$ subsets were analyzed for BrdU incorporation and $K_i$-67 expression 24 h after injection of 2 mg BrdU. (*A*) Representative FACS plots. All dot plots show gated α-GalCer-CD1d tetramer$^{+}$ TCR-β$^{+}$ iNKT cells. (*Left*) All iNKT cells. (*Center*) NK1.1$^{-}$ CD44$^{+}$ CD24$^{-}$ subset. (*Right*) NK1.1$^{-}$ CD44$^{-}$ CD24$^{+}$ subset. (*B*) Cumulative data for the NK1.1$^{-}$ CD44$^{+}$ CD24$^{-}$ (*Top*) and NK1.1$^{-}$ CD44$^{-}$ CD24$^{+}$ (*Bottom*) iNKT cell subsets. One representative experiment of two; $n$ = 3. (*C* and *D*) Autophagy-deficient T cells are more susceptible to apoptosis. Thymocytes (*C* and *D*) and splenocytes (*C*) of WT and CD4 Cre-Atg7$^{-/-}$ mice (*C*) or control (SJL:WT)

Legend continued on following page

and SJL:CD4 Cre-Atg7$^{-/-}$ chimeras (*D*) were stained ex vivo with Annexin V antibodies to detect apoptotic cells. Depicted are the percentages (mean ± SD) of apoptotic iNKT cells. (*E* and *F*) Impaired expansion of CD4 Cre-Atg7$^{-/-}$ thymic iNKT cells in response to α-GalCer. (*E*) CSFE-labeled thymocytes were incubated with vehicle or α-GalCer as described in *Materials and Methods*. Fold expansion was calculated as percentage of iNKT cells at day 4/input percentage of iNKT cells. Population expansion in vehicle controls is likely due to the presence of IL-2 and IL-7 in the culture medium. (*F*) Representative dot plots depicting CFSE staining and CD25 expression on iNKT cells (*Left*) and CD8 cells (*Right*) of WT (*Top*) and CD4 Cre-Atg7$^{-/-}$ thymocytes (*Bottom*) upon vehicle or α-GalCer stimulation. FACS plots of the same samples are shown in *E*.

**Fig. S6.** Reduced frequency of mature peripheral T cells in CD4 Cre-Atg7$^{-/-}$ mice. (*A*) Percentages of naive, memory, effector memory (EM), and central memory (CM) T cells (mean ± SD) in the spleen of WT or Cre-Atg7$^{-/-}$ mice. $n = 4$ mice/group. (*B*) Expression of CD62L and CD44 on splenic CD4 and CD8 T cells and quadrants used to identify naive, memory, EM, and CM populations. (*C*) MFI (mean ± SD) of Mitotracker green staining of WT splenocytes. $n = 4$ mice/group; shown is one experiment representative of four.

**Fig. S7.** Representative FACS dot plots depicting CD62L and CD44 expression on CD4 and CD8 cells in the spleen and liver of bone marrow chimeric mice. Shown are the plots of CD45.1- and CD45.2-positive cells in control SJL:WT and CD4 Cre Atg7$^{-/-}$ chimeric mice.

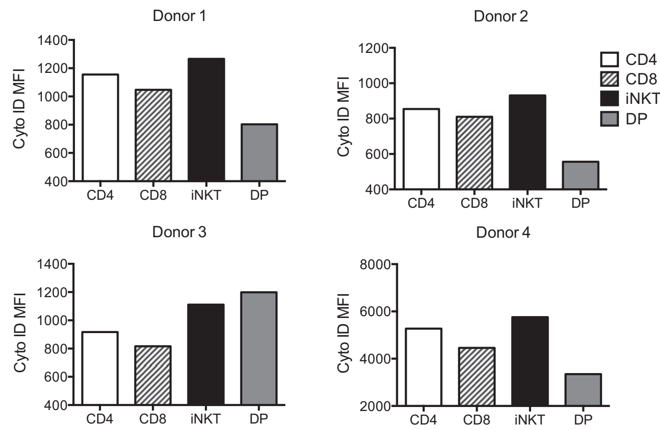


**Fig. S8.** MFI values for Cyto ID staining of the four human thymuses described in Fig. 8.

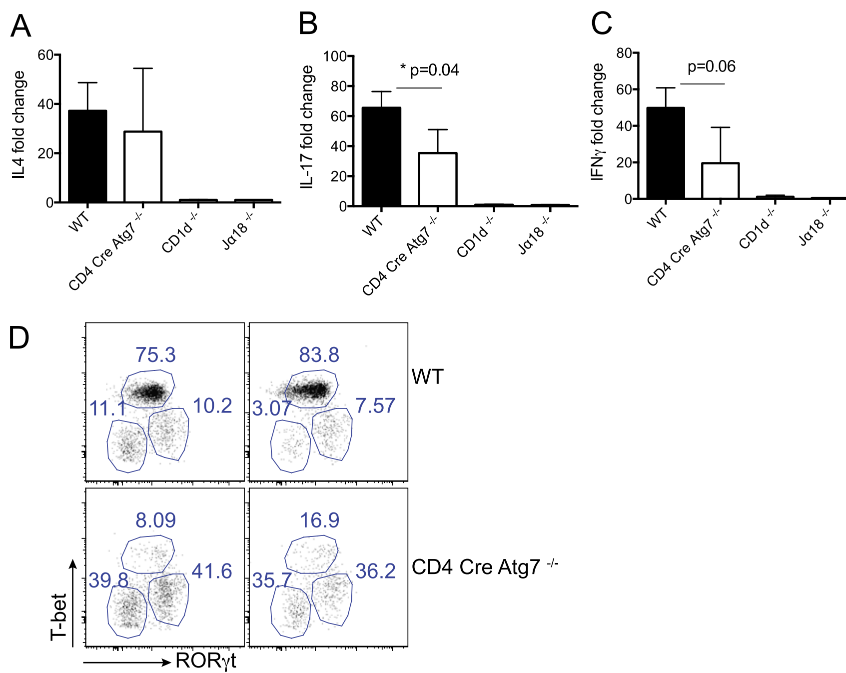


**Fig. S9.** Impairment of NKT-1 and NKT-17 iNKT cell subsets in CD4 Cre-Atg7$^{-/-}$ mice. (*A*–*C*) Fold change of IL-4 (*A*), IL-17 (*B*), and IFN-γ (*C*) in supernatants of thymocytes stimulated for 4 d with α-GalCer (iNKT cell fold expansion of the same cultures is shown in Fig. S5*E*). Black bars, WT mice; white bars, CD4 Cre-Atg7$^{-/-}$ mice. Negative controls were CD1d$^{-/-}$ and Jα18$^{-/-}$ mice. Pooled data from two experiments; *n* = 4–5 mice/group. (*D*) Representative plots depicting intracellular staining with antibodies to T-bet and RORγt in two WT and two CD4 Cre-Atg7$^{-/-}$ mice.